Journal of Pharmaceutical and Biomedical Analysis 51 (2010) 1060–1063

Contents lists available at ScienceDirect

Journal of Pharmaceutical and Biomedical Analysis

journal homepage: www.elsevier.com/locate/jpba

Determination of potency of heparin active pharmaceutical ingredient by near infrared reflectance spectroscopy

Chunxiao Sun [a], Hengchang Zang [a,*], Xiumei Liu [a], Qin Dong [a], Lian Li [a], Fengshan Wang [a], Linyan Sui [b]

[a] National Glycoengineering Research Center and College of Pharmacy, Shandong University, 250012 Jinan, China
[b] Jin Hongli Apparatus Company of Jinan, 250012 Jinan, China

ARTICLE INFO

Article history:
Received 21 June 2009
Received in revised form 21 October 2009
Accepted 24 November 2009
Available online 1 December 2009

Keywords:
NIRS
SG-1st derivative
Heparin API
Potency

ABSTRACT

Potency is an important parameter for evaluation of quality of heparin active pharmaceutical ingredient (API). In this paper the feasibility to determine potency of heparin API with near infrared reflectance spectroscopy (NIRS) coupled with partial least squares (PLS) algorithm is attempted. PLS factors, correlation coefficient of calibration set (R_c), the root mean square of cross-validation (RMSECV), correlation coefficient of prediction set (R_p) and the root mean square of prediction (RMSEP) were used to evaluate the performance of the models. The optimal calibration model was obtained with $R_p = 0.9721$ and RMSEP = 0.55 in the 1700–1898 nm spectral region when using SG-1st derivative spectral transform method and division of calibration/prediction samples was 1/1. Three other additional samples demonstrated good prediction capability of the final model and three validation samples gave good repeatability result. NIRS has the potential to be a final lot release test to be performed in a QC laboratory.

1. Introduction

Heparin is a primary implemented anticoagulant used for life-saving medical therapies for more than 75 years [1–3]. It is a polydisperse mixture of polysaccharides containing disaccharide repeating units of glucuronic–iduronic acid linked to glucosamine, belonging to the family of glycosaminoglycans (GAGs) [4,5]. Heparin is isolated by extraction from animal organs, tissues and cells, such as porcine intestines [6]. Anticoagulant activity, namely potency, is an important parameter for evaluation of quality of heparin. Various methods can be applied to determine the potency of heparin API, such as plasma-based assays and colorimetric methods. However, all these methods are reagent-consuming and time-wasting.

As a fast and non-destructive method, near infrared reflectance spectroscopy (NIRS) has been reported to be successfully applied in the pharmaceutical industry; see reviews [7,8].

NIR spectra are mainly composed of overtone and combination bands and absorption in NIR region is primarily due to hydrogen stretching vibrations, involving C–H, O–H and N–H containing functional groups [9]. Many of these are present in heparin molecules and hence NIRS is suitable to study the physical or chemical properties of heparin. Spencer et al. [10] used NIRS to develop PLS models for heparin API's three major components: heparin, oversulfated chondroitin sulfate (OSCS) and GAGs, demonstrating the feasibility of NIRS to identify contamination of heparin. However, to the best of our knowledge, there are no reports using NIRS to study the potency of heparin API.

Pretreatment of crude spectral data is important because the NIR spectra are often influenced by instrumental variation and measurement conditions, causing background noise and baseline drift [11]. There are different spectral pretreatment methods, among which SG can be used effectively for smoothing high-frequency noise and elevating signal-to-noise ratio. The 1st derivative can eliminate translation and baseline drift, wipe out interference of other background, discriminate overlapping peaks and improve resolution and sensitivity of spectra [12]. Second derivative makes it easier to see the peak feature in the raw spectrum. Both SNV and MSC can remove slope variation and correct light scatter due to different particle sizes [13–16]. Division of calibration/prediction samples and spectral regions also exert influence on calibration.

The objective of this study was to demonstrate the applicability of NIRS for the determination of the potency of heparin API and compare the impact of different spectral pretreatment methods, division of calibration/prediction samples and spectral regions on the performance of the models. PLS factors, correlation coefficient of calibration set (R_c), the root mean square of cross-validation (RMSECV) and correlation coefficient of prediction set (R_p), the root mean square of prediction (RMSEP) were used to evaluate the performance of the models.

* Corresponding author. Tel.: +86 531 88380288; fax: +86 531 88380288.
E-mail address: zanghcw@126.com (H. Zang).

0731-7085/$ – see front matter © 2009 Elsevier B.V. All rights reserved.
doi:10.1016/j.jpba.2009.11.022

Table 1
Background information of the three batches of factory heparin API samples.

Batch no.	Potency (IU/mg)	wt.% OSCS	wt.% water
0807004	162	0.0	2.3
0808005	154	0.0	1.8
0809004	160	0.0	1.9

2. Materials and methods

2.1. Sample preparation

Three batches of heparin API samples were obtained from Zaozhuang Sai Nuokang Biochemical Limited Company of Shandong province in China. Background information of these is shown in Table 1. ^{1}H NMR and CE methods demonstrated that there was no known adulterant-oversulfated chondroitin sulfate (OSCS) in the samples. The water content was determined by weight loss on drying method. To obtain more samples of different potencies, we created other six batches by mixing the original three batches of samples with different ratios. Thus nine batches, a total of 44 groups of samples were obtained. The samples were stored in a desiccator and comminuted by a factory bucker in about 1 min resulting in a powder with a grain size of about 180 μm.

2.2. Chemical analysis

The potency of each sample was measured by caprine blood plasma method according to United States Pharmacopeia [17]. Each sample was measured three times, and the average value was used. Results showed that there were 7 different potencies, namely 154, 156, 157, 158, 159, 160 and 162.

2.3. NIR measurement

NIR measurement was carried out using Brimrose Luminar 5030 AOTF-NIR spectrometer (Brimrose Co., USA) with an InGaAs detector. NIR spectra were collected at room temperature (about 22 °C); the humidity was steady in the laboratory. Each spectrum was the average of 300 scans with a wavelength increment of 2 nm over the wavelength range 1100–2300 nm. The diffuse reflectance spectra of the samples were collected in ratio mode. The sample cup could contain approximately 5 mg sample at the bottom of which there was an optical reflector, which reflects back NIR radiation to the detector. The sample was compressed when the cup was closed by a cap, in the center of which there was a hole, through which the NIR radiation could pass into the sample. Two spectra of each sample were collected and then the averaged spectrum was calculated. Therefore, a total of 44 spectra were obtained, each spectrum has 601 data points. Brimrose Snap! 2.03 software was used for spectra acquisition.

2.4. Sample dividing

Potency of each heparin API sample was assigned to corresponding spectrum data. Then, principal component analysis (PCA) was performed to help divide samples to construct calibration set and prediction set, which are used for model construction and validation, respectively. For example, there were 8 samples with potency of 160, which were arranged orderly from up to down in the PCA plot, then 5 samples were selected uniformly from those 8 samples to consist the calibration set. So 29 samples were selected uniformly to consist calibration set, the left 15 samples then made up the prediction set, thus a 2/1 division of calibration/prediction samples was obtained. Then a 1/2 division was got through exchange of the above two sets and a 1/1 division was obtained by selecting 22 samples to form calibration set with 22 samples left consisting the prediction set. 2/1 was first selected because this is the generally accepted division for good modelling. However, a total of 44 samples are not representative enough to fully exert the validation function, so 1/2 and 1/1 division was then used for modelling to compare the results. All these were performed in the Unscrambler software, version 7.8 (Camo process AS).

2.5. Spectral transforms

All the 44 raw spectra were transformed so that the baseline offset, slope variation and some noise could be removed and corrected. Four spectra transform methods were applied to compare their effects on calibration. They were SG-1st derivative with 5 smoothing points, SG-2nd derivative with 5 smoothing points, SNV and MSC. When taking MSC, an average spectrum of all 44 samples was firstly obtained to create an “ideal spectrum”. All of the pretreatment methods were also taken in Snap! 2.03 software.

2.6. Spectral regions

The full spectral region ranging from 1100 to 2300 nm was split into 6 equidistant parts to compare calibration results, namely 1100–1298 nm, 1300–1498 nm, 1500–1698 nm, 1700–1898 nm and 1900–2100 nm.

2.7. Models calibration and validation

Partial least squares (PLS) method was used in the Unscrambler software to construct calibration models. Once the calibration models were created, they were applied to prediction set for validation.

2.8. Prediction capability and repeatability

Three additional OSCS-free samples supplied by the same factory were used to inspect the prediction capability of the final PLS model. Their potencies were also measured by caprine blood plasma method. Three validation samples with different potencies were measured 10 times without any moving; the mean potencies and standard deviation were calculated.

3. Results and discussion

3.1. Raw spectra

Fig. 1 shows the raw spectra of all the 44 samples. Two bands at 1400–1450 nm and 1900–1950 nm are due to strong absorption of water [18], which is allowed to be present up to 5% (w/w) in heparin API. Light scattering caused by different particle size and density affected the raw spectra, resulting in baseline drift.

3.2. Score plots and sample sets information

Fig. 2 shows score plots of the spectra. The 44 samples were arranged in order of potency of heparin API. From left to right, the potencies were 154, 156, 157, 158, 159, 160 and 162 respectively, suggesting that PC1 represented the information of potency. Concrete sample sets information of 2/1 and 1/1 division of calibration/prediction samples were shown in Table 2. As seen, the potency range and distribution of both calibration set and prediction set were balanced and representative.

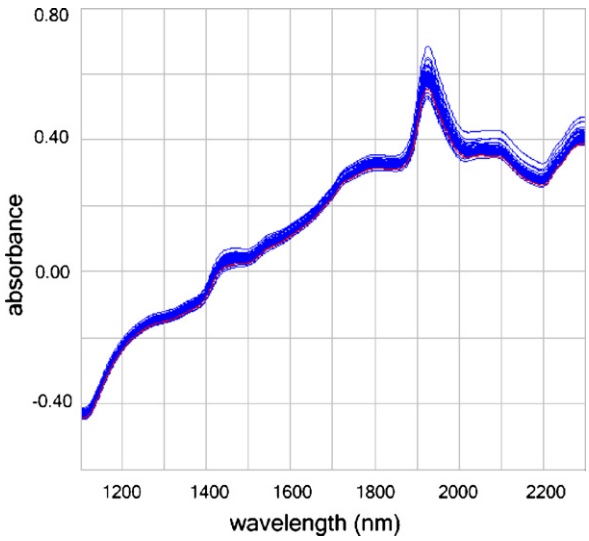

Fig. 1. Raw spectra of 44 samples.

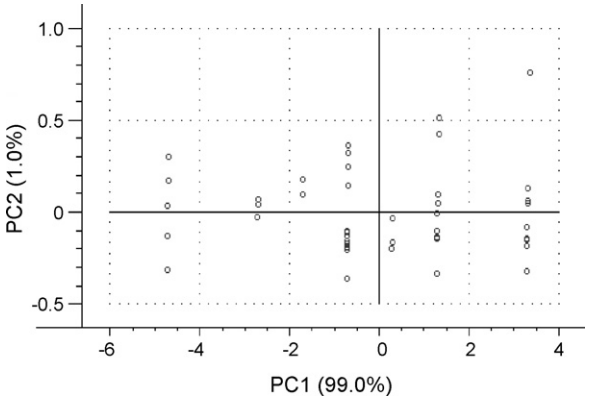

Fig. 2. Score plot of the 44 spectra.

3.3. PLS models for potency of heparin API

After leave-one-out cross-validation, a lowest RMSECV was obtained and the corresponding number of PLS factors was the optimal. Correlation coefficients (R) for the measured and predicted values were calculated for both calibration set and prediction set. Correlation coefficient of prediction set (R_p) and the root mean square of prediction (RMSEP) were the most important parameters for evaluating the performance of the models.

3.3.1. Impact of spectra transform methods

The impact of spectra transform methods on performance of models constructed in full spectral region with a 2/1 division of calibration/prediction samples is shown in Table 3. It can be seen that comparing to model without any transform, the model through

Table 2
Sample sets information with different division of calibration/prediction samples.

Division	Sample set	Units	n[a]	Range	Mean	SD[b]
2/1	Calibration	IU/mg	29	154–162	158.79	2.43
	Prediction	IU/mg	15	154–162	158.53	2.59
1/1	Calibration	IU/mg	22	154–162	158.41	2.54
	Prediction	IU/mg	22	154–162	159.00	2.39

[a] n = number of samples.
[b] SD = standard deviation.

Table 3
Parameters of models under different spectral transform methods in full spectral region with a 2/1 division of calibration/prediction samples.

Preprocessing method	n[a]	PLS factors	R_c[b]	RMSECV	R_p[c]	RMSEP
No preprocessing	28	4	0.8508	1.24	0.8996	1.11
SG-1st derivative	29	6	0.9525	0.73	0.9823	0.49
SG-2nd derivative	28	2	0.8391	1.28	0.9201	0.99
SNV	28	5	0.8764	1.14	0.8351	1.38
MSC	28	1	0.8508	1.23	0.8944	1.13

[a] n = number of samples for calibration.
[b] R_c = correlation coefficient of calibration set.
[c] R_p = correlation coefficient of prediction set.

SG-1st derivative spectral transform gave the highest R_p and the lowest RMSEP, thus it was the best spectra transform method for measuring potency of heparin API. However, except SNV, other results all obviously showed that RMSEP < RMSECV, this was abnormal to some extent. The reason for this could be that the number of 15 samples in prediction set was too low so that they were not representative enough to fully exert the validation function.

3.3.2. Impact of division of calibration/prediction samples

Then, 1/2 and 1/1 divisions of calibration/prediction samples were used to construct models in full spectral region with SG-1st derivative transform. Results were presented in Table 4. Results of RMSEP > RMSECV indicated that samples in prediction set had fully exercised their validation function. What is more, models with 1/1 division gave higher R_p and lower RMSEP, thus in condition of total 44 samples, the 1/1 division of calibration/prediction samples was best for calibration. However, the PLS factors of 7 was somewhat too high.

3.3.3. Impact of spectral regions

The full spectral region ranging from 1100 to 2300 nm was split into 6 equidistant parts. Then PLS models were constructed with SG-1st derivative transform and 1/1 division of calibration/prediction samples in every region, results showed that model constructed in 1700–1898 nm gave a higher R_p (0.9721) and a lower RMSEP (0.55), and the PLS factor was reduced to 4. This is because the noise in the range of 1700–1898 nm is less while effective information is relatively more than in other spectral regions. Results of the restricted range study also were placed in Table 4. Correlation plot of calibration set in the final model was presented in Fig. 3.

3.4. Prediction capability and repeatability

The three additional samples were proved to comply with the tested parameter using the PCA model, which was presented in Fig. 4, so they could be predicted by the final model. After SG-1st

Table 4
Parameters of models with SG-1st derivative spectral transform method and different division of calibration/prediction samples in different spectral regions.

Spectral region (nm)	Division	n[a]	PLS factors	R_c	RMSECV	R_p	RMSEP
1100–2300	1/2	15	6	0.9748	0.58	0.9385	0.83
1100–2300	1/1	22	7	0.9710	0.60	0.9705	0.61
1100–1298	1/1	22	5	0.8664	1.27	0.8184	1.46
1300–1498	1/1	22	6	0.8166	1.45	0.9258	0.89
1500–1698	1/1	22	5	0.9595	0.78	0.9557	0.73
1700–1898	1/1	22	4	0.9678	0.57	0.9721	0.55
1900–2098	1/1	22	2	0.7673	1.60	0.8264	1.43
2100–2300	1/1	22	2	0.7800	1.56	0.8420	1.40

[a] n = number of samples for calibration.

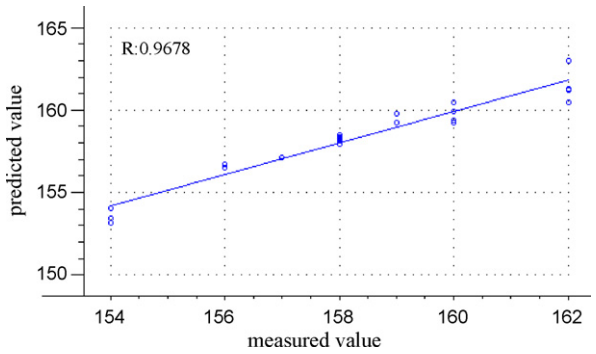

Fig. 3. Correlation plot of calibration set between the measured and predicted values obtained with SG-1st derivative spectra preprocessing method and 1/1 division of calibration/prediction samples in the spectral region of 1700–1898 nm.

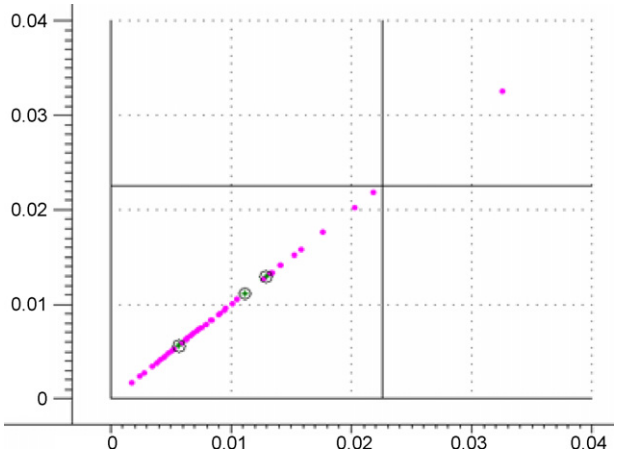

Fig. 4. Tested by PCA, the additional three samples (marked with larger rings) were demonstrated to comply with the tested parameter.

Table 5
Predicted values, measured values and recoveries of three additional samples.

Sample number	Predicted value	Measured value	Recovery
1	158.51	159	99.69%
2	160.60	161	99.75%
3	158.15	158	100.09%

Table 6
Repeatability results for 10 repeated readings of three validation samples.

Number	Potency (IU/mg)	Mean	SD[a]
1	160	159.77	0.26
2	156	156.83	0.39
3	159	158.36	0.11

[a] SD = standard deviation.

derivative transform of original spectra, region of 1700–1898 nm was used for predicting. Predicted values, measured values and recoveries were shown in Table 5. It can be seen that recoveries were near to 100%, indicating good prediction capability of the final model. Repeatability results were shown in Table 6. The three validation samples gave an overall value of 0.25 IU/mg for repeatability of heparin API.

4. Conclusion

The overall results demonstrated that potency of heparin API could be determined non-destructively by NIRS with PLS algorithm. Comparing models constructed with SG-1st derivative, SG-2nd derivative, SNV and MSC spectral transform methods to model constructed without any pretreatment, SG-1st derivative performed best. The optimal calibration model was obtained with $R_p = 0.9721$ and RMSEP = 0.55 in the 1700–1898 nm spectral region when division of calibration/prediction samples was 1/1. Three other additional samples demonstrated good prediction capability of the final model and three validation samples gave good repeatability results. As a fast and non-destructive analytical tool, NIRS has the potential to improve the quality of the drug manufacturing process from incoming raw materials to the final drug product. This article demonstrated the possibility to determine potency of heparin API with NIRS, indicating its potential to be a final lot release test to be performed in a QC laboratory.

Acknowledgements

We are grateful for financial support from National Glycoengineering Research Center of China and Department of Science & Technology of Shandong Province. We also thank Zaozhuang Sai Nuokang biochemical limited company of Shandong province, for the supply of heparin API samples and Jin Hongli Apparatus Company of Jinan, for free use of AOTF-NIR spectrometer.

References

[1] C. Longstaff, C.M. Whitton, R. Stebbings, E. Gray, How do we assure the quality of biological medicines? Drug Discov. Today 14 (2009) 50–55.
[2] B. Li, J. Suwan, J.G. Martin, F. Zhang, Z. Zhang, D. Hoppensteadt, M. Clark, J. Fareed, R.J. Linhardt, Oversulfated chondroitin sulfate interaction with heparin-binding proteins: new insights into adverse reactions from contaminated heparins, Biochem. Pharmacol. 78 (2009) 292–300.
[3] I. Capila, R.J. Linhardt, Heparin–protein interactions, Angew. Chem. Int. Ed. Engl. 41 (2002) 391–412.
[4] N. Volpi, F. Maccari, R.J. Linhardt, Capillary electrophoresis of complex natural polysaccharides, Electrophoresis 29 (2008) 3095–3106.
[5] N. Volpi, F. Maccari, R.J. Linhardt, Quantitative capillary electrophoresis determination of oversulfated chondroitin sulfate as a contaminant in heparin preparations, Anal. Biochem. 388 (2009) 140–145.
[6] R.J. Linhardt, N.S. Gunay, Production and chemical processing of low molecular weight heparins, Semin. Thromb. Hemost. 25 (1999) 5–16.
[7] J. Luypaert, D.L. Massart, Y. Vander Heyden, Near-infrared spectroscopy applications in pharmaceutical analysis, Talanta 72 (2007) 865–883.
[8] Y. Roggo, P. Chalus, L. Maurer, C. Lema-Martinez, A. Edmond, N. Jent, A review of near infrared spectroscopy and chemometrics in pharmaceutical technologies, J. Pharm. Biomed. Anal. 44 (2007) 683–700.
[9] Y. Huang, J. Tang, B.G. Swanson, A.G. Cavinato, M. Lin, B.A. Rasco, Near infrared spectroscopy: a new tool for studying physical and chemical properties of polysaccharide gels, Carbohydr. Polym. 53 (2003) 281–288.
[10] J.A. Spencer, J.F. Kauffman, J.C. Reepmeyer, C.M. Gryniewicz, W. Ye, D.Y. Toler, L.F. Buhse, B.J. Westenberger, Screening of heparin API by near infrared reflectance and Raman spectroscopy, J. Pharm. Sci. 98 (2009) 3540–3547.
[11] D. Zhu, B. Ji, C. Meng, B. Shi, Z. Tu, Z. Qing, The application of direct orthogonal signal correction for linear and non-linear multivariate calibration, Chemometr. Intell. Lab. Syst. 90 (2008) 108–115.
[12] Z. Ni, C. Hu, F. Feng, Progress and effect of spectral data pretreatment in NIR analytical technique, Chin. J. Pharm. Anal. 28 (2008) 824–829.
[13] Q. Chen, J. Zhao, M. Liu, J. Cai, J. Liu, Determination of total polyphenols content in green tea using FT-NIR spectroscopy and different PLS algorithms, J. Pharm. Biomed. Anal. 46 (2008) 568–573.
[14] L. Liu, L. Huang, Y.L. Yan, Z.Y. Wang, Progress in the study of impact of scattering on stability of quantitative analysis model using near infrared spectroscopy technology and correction methods, Guang Pu Xue Yu Guang Pu Fen Xi 28 (2008) 2290–2295.
[15] P. Geladi, D. MacDougall, H. Martens, Linearization, Scatter-correction for near-infrared reflectance spectra of meat, Appl. Spectrosc. 39 (1985) 491–500.
[16] R.J. Barnes, M.S. Dahnoa, S. Lister, Standard normal variate transformation and de-trending of near-infrared diffuse reflectance spectra, Appl. Spectrosc. 43 (1989) 772–777.
[17] USP XX.1990, 632.
[18] Y. Zheng, X. Lai, S.W. Bruun, H. Ipsen, J.N. Larsen, H. Løwenstein, I. Søndergaard, S. Jacobsen, Determination of moisture content of lyophilized allergen vaccines by NIR spectroscopy, J. Pharm. Biomed. Anal. 46 (2008) 592–596.